

1 **Supplementary Information accompanying the manuscript titled:**

2
3 “Dual clumped isotopes from Mid-Eocene bivalve shell reveal a hot and
4 summer wet climate of the Paris Basin”

5
6 Jorit F. Kniest^{1*}, Amelia J. Davies¹, Julia Brugger², Jens Fiebig¹, Miguel Bernecker¹,
7 Jonathan A. Todd³, Thomas Hickler², Silke Voigt¹, Alan Woodland¹, Jacek Raddatz^{1,4}

8 ¹ Institute for Geoscience, Goethe-University, Frankfurt a.M., Germany

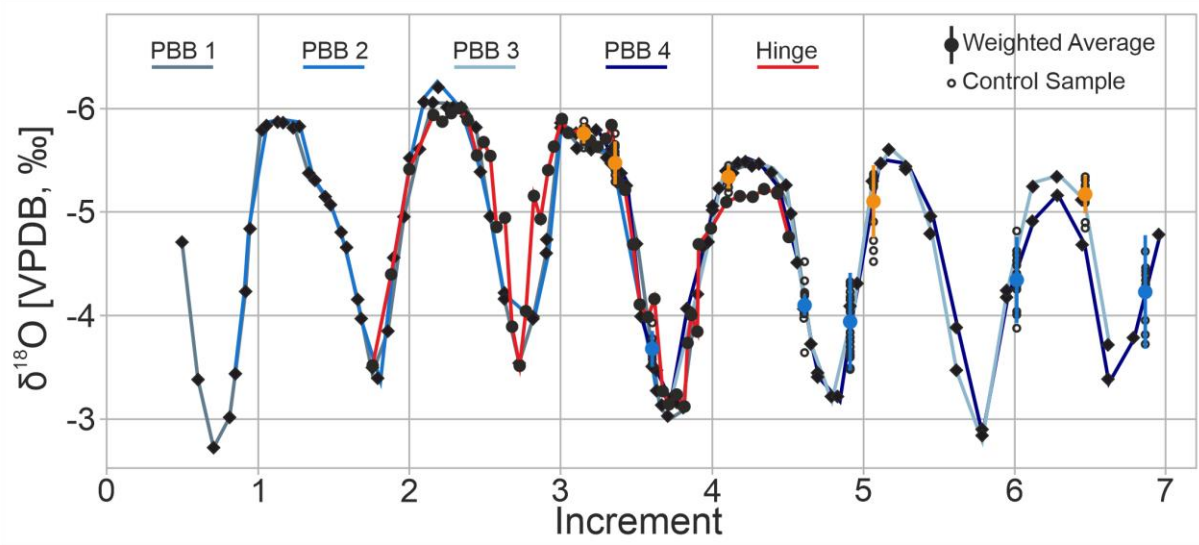
9 ² Department of Biogeography and Ecosystem Ecology, Senckenberg Institute and Natural History
10 Museum, Frankfurt a.M., Germany

11 ³ Department of Earth Sciences, The Natural History Museum, London, UK

12 ⁴ GEOMAR Helmholtz Centre for Ocean Research Kiel, Kiel, Germany

13 * Corresponding Author (kniest@em.uni-frankfurt.de)

14
15 Submitted for publication to Nature Communications in Earth and Environment



35
36 **Fig. S1 – Comparison of stable oxygen isotope variability of parallel shell sections –**
37 $\delta^{18}\text{O}_c$ values (black diamonds) and corresponding shell sections (PBB1 to PBB4) are
38 superimposed as a master record of the shell (Supplementary data 1). Additionally, sampling
39 positions for the dual clumped isotope analyses are shown with the $\delta^{18}\text{O}_c$ values of the
40 individual control samples (black rings) and their weighted averages ($\pm 2\sigma$) (Supplementary
41 data 2). The colour code of each position corresponds to the subsequent compiled bulk sample
42 (BL – orange; BH - blue).

43

44

45

46

47

48

49

50

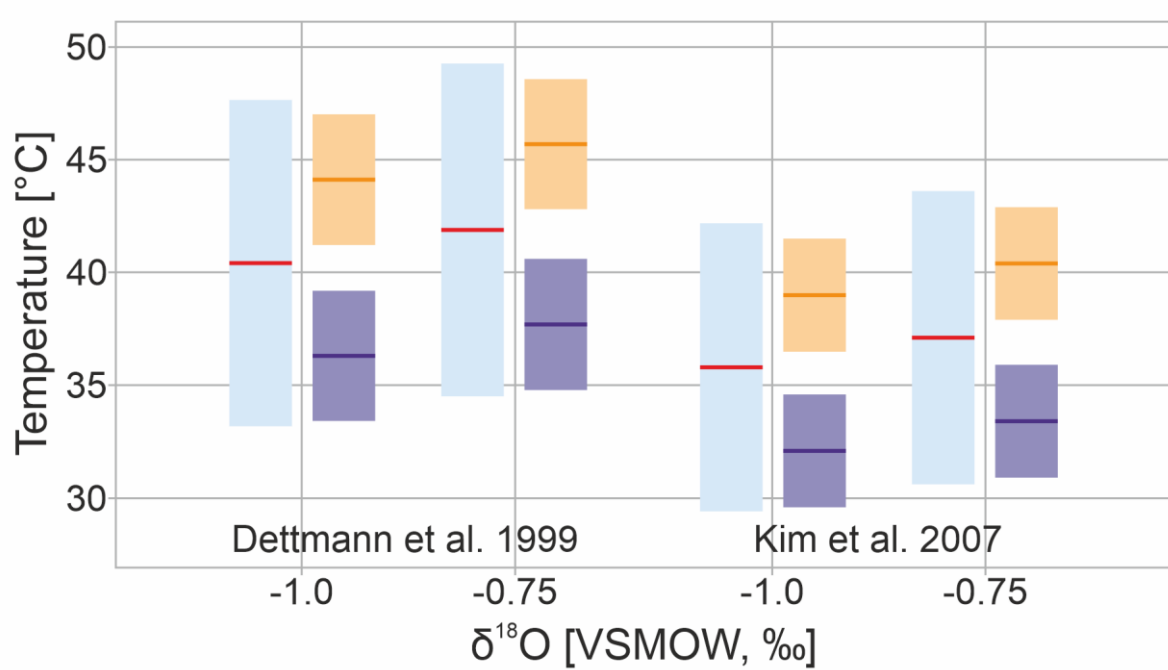
51

52

53

54

55



56

57

58 **Fig. S2– Comparison of temperature reconstructions in dependence of calibration and**
 59 **sea water isotopic composition** – Water temperatures reconstructions from $\delta^{18}\text{O}_\text{C}$ values are
 60 presented depending on the used carbonate-water-fractionation calibration (Dettmann et al.³,
 61 Kim et al.⁴) and $\delta^{18}\text{O}_\text{SW}$ of -1.0 and -0.75‰ (VSMOW). Seasonal amplitude (light blue box) and
 62 MAT (red line) are derived from the non-linear regression model. The weighted average ($\pm 2\sigma$)
 63 of the two bulk samples are display as the orange (BL), respectively, dark blue (BH) boxes.

64

65

66

67

68

69

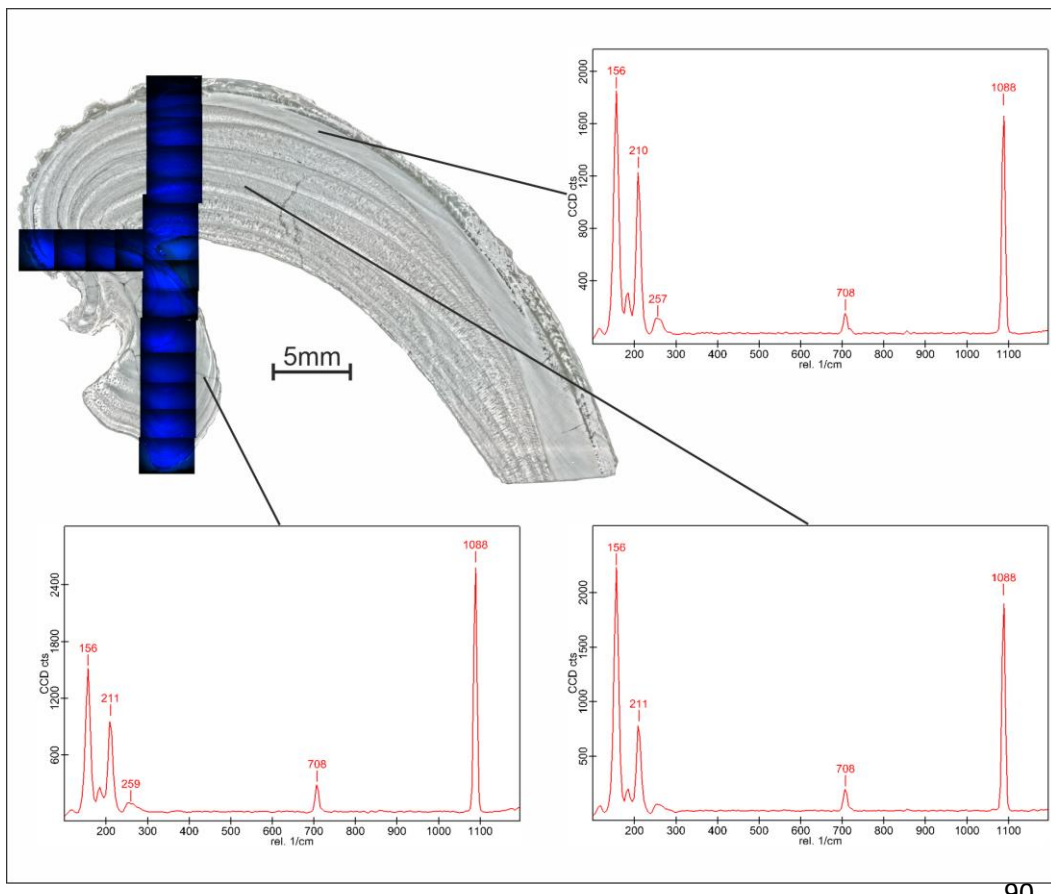
70

71

72

73

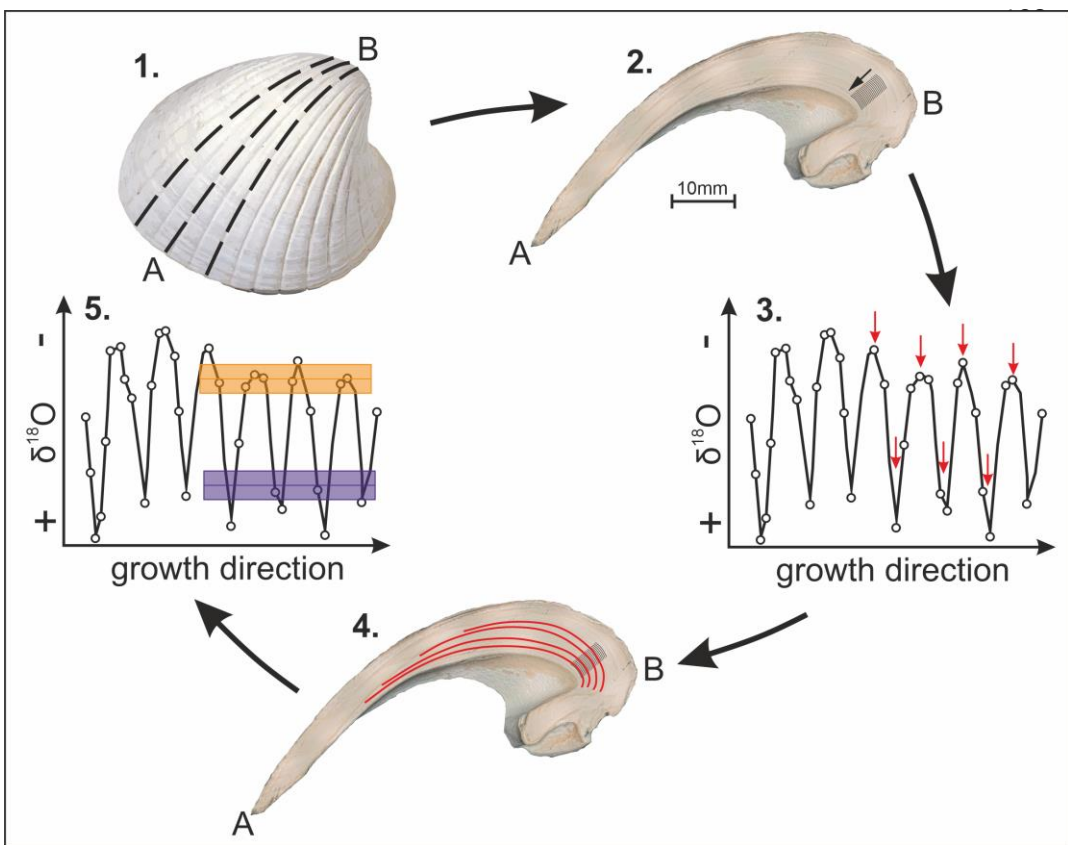
74



90

Fig. S3 – Cathodoluminescence and Raman spectra of selected shell parts – CL is carried out with overlapping imaging along two axes of the shell, revealing a dim blue luminescence for the analysed area. Raman spectroscopy exclusively show characteristic aragonite spectra with distinct double peaks at 156 and 211 cm^{-1} .

91
92
93
94
95
96
97
98
99
100
101
102
103
104
105
106
107



123

124 **Fig. S4 – Material sampling routine for isotope analysis** – 1. Cutting a plane parallel to the
 125 maximum growth axis of the shell; 2. Sampling inner shell area along the growth direction for
 126 stable isotopes; 3. Identifying annual extrema in the shell isotope record; 4. Resampling longer
 127 tracks along the inner shell for the dual clumped analysis; 5. Combing the material to two bulk
 128 samples, which represent the lighter, respectively, heavier section of the isotopic record; Steps
 129 1 to 4 are repeated for shell planes PBB1 to PBB4, in order to match the necessary sample
 130 amount for step 5.

131

132

133

134

135

136

137

138

139

140

141

142

143

144

145

146

147

148

149

150

151

152

153

154

155

156

157

158

159

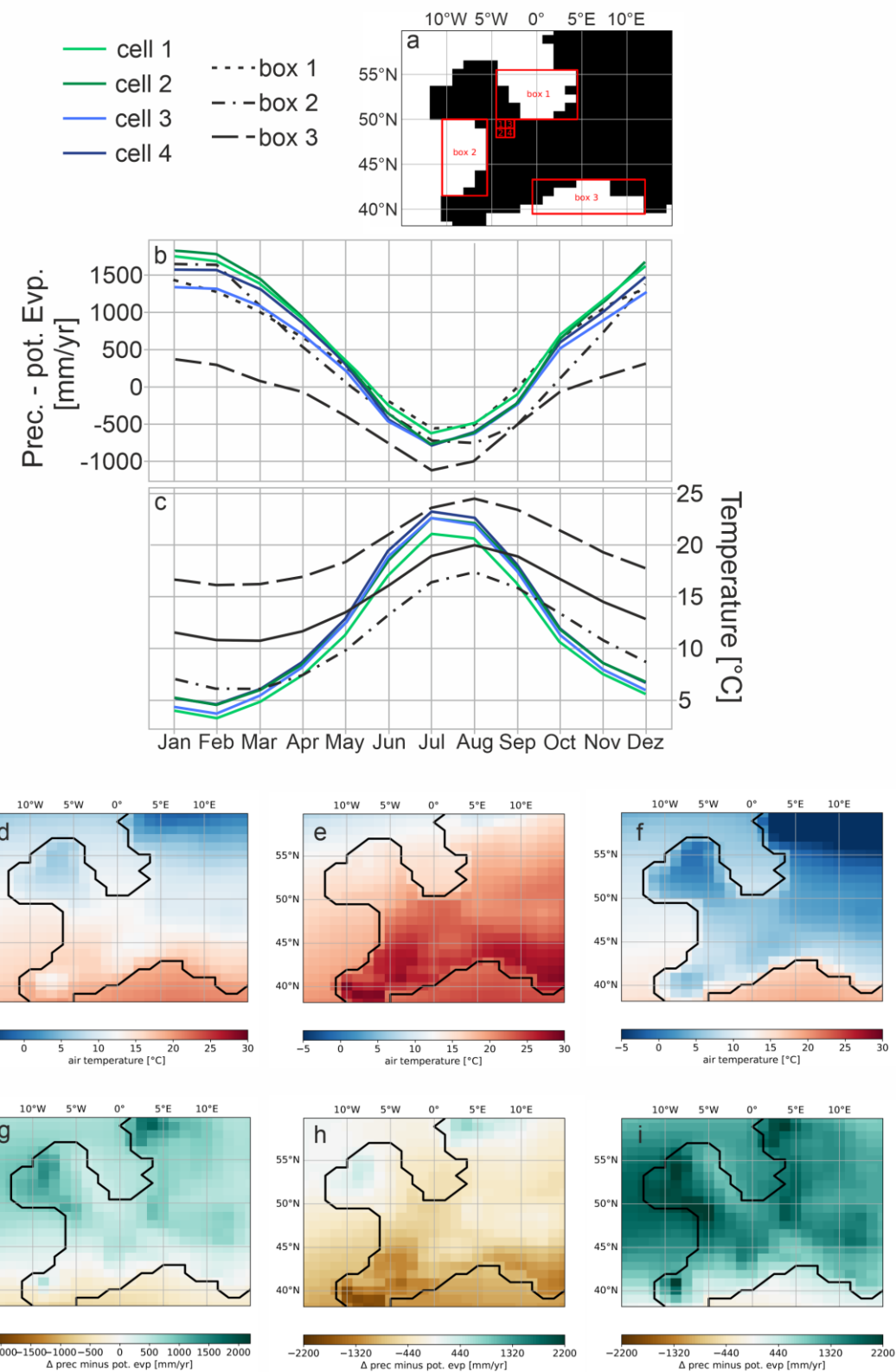
160

161

162

163

164

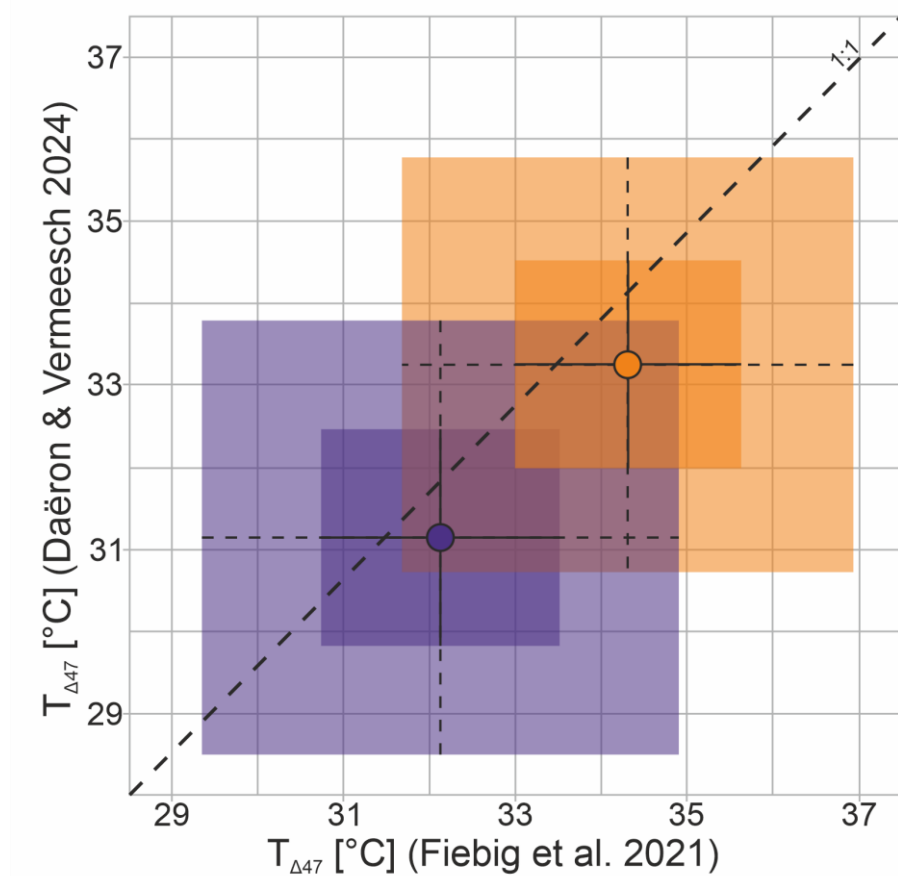


165 **Fig. S5 - Climate model derived distribution of temperature and precipitation minus**
166 **evapotranspiration** – Seasonal distribution of air temperature and precipitation minus
167 evapotranspiration for western Europe during the MECO (40Ma) derived from the compiled
168 dataset of Li et al.² using the Community Earth System Model (CESM1.2.2). (a) Paleo-
169 geography and selected continental cells and marginal sea basins; (b and c): Seasonal
170 distribution of air temperature and precipitation minus evapotranspiration for box 1 to 3 and
171 cell 1 to 4; (d to f): annual mean, summer and winter air temperatures; (g to i): annual mean,
172 summer and winter precipitation minus potential evapotranspiration

173

174

175



176

177 **Fig. S6 – Comparison of Δ_{47} -temperature calibration output** – Δ_{47} values of BL (orange
178 box) and BH (blue box) are converted into temperatures using the calibrations of Fiebig et al.⁵
179 and Daëron & Vermeesch⁶. Uncertainties for Δ_{47} measurements are fully error propagated and
180 represent 68% (solid line) and 95% (dashed line) confidence intervals. The dashed black line
181 indicates the proposed 1:1-relationship between the two temperature reconstructions.

182 **References**

- 183 1. Huyghe, D., Lartaud, F., Emmanuel, L., Merle, D. & Renard, M. Palaeogene climate evolution in
184 the Paris Basin from oxygen stable isotope ($\delta^{18}\text{O}$) compositions of marine molluscs. *JGS* **172**,
185 576–587; 10.1144/jgs2015-016 (2015).
- 186 2. Li, X. *et al.* A high-resolution climate simulation dataset for the past 540 million years. *Scientific
187 data* **9**, 371; 10.1038/s41597-022-01490-4 (2022).
- 188 3. Dettman, D. L., Reische, A. K. & Lohmann, K. C. Controls on the stable isotope composition of
189 seasonal growth bands in aragonitic fresh-water bivalves (unionidae). *Geochimica et
190 Cosmochimica Acta* **63**, 1049–1057; 10.1016/S0016-7037(99)00020-4 (1999).
- 191 4. Kim, S.-T., O’Neil, J. R., Hillaire-Marcel, C. & Mucci, A. Oxygen isotope fractionation between
192 synthetic aragonite and water: Influence of temperature and Mg²⁺ concentration. *Geochimica
193 et Cosmochimica Acta* **71**, 4704–4715; 10.1016/j.gca.2007.04.019 (2007).
- 194 5. Fiebig, J. *et al.* Calibration of the dual clumped isotope thermometer for carbonates. *Geochimica
195 et Cosmochimica Acta* **312**, 235–256; 10.1016/j.gca.2021.07.012 (2021).
- 196 6. Daëron, M. & Vermeesch, P. Omnivariant Generalized Least Squares regression: Theory,
197 geochronological applications, and making the case for reconciled $\Delta 47$ calibrations. *Chemical
198 Geology* **647**, 121881; 10.1016/j.chemgeo.2023.121881 (2024).

199